CFD Simulation of an Unconfined Vapor Cloud Explosion through obstacles using OpenFoam

Cléante Langree, E. Franquet, J. Reveillon, Guillaume Lecocq, F.X. Demoulin

CFD Simulation of an Unconfined Vapor Cloud Explosion through obstacles using OpenFoam®

C. Langrée[a,b], E. Franquet[c], J. Reveillon[a], G. Lecocq[b] & F.X. Demoulin[a]

[a] Complexe de Recherche Interprofessionnel en Aérothermochimie (CORIA), Rouen, France
[b] Institut National de l'Environnement Industriel et des Risques (INERIS), Verneuil en halatte, France
[c] Laboratoire de Thermique, Energétique et Procédés (LaTEP), Pau, France

E-mail: *langreec@coria.fr*

Abstract

In this work, numerical simulations are carried out to characterize the impact of obstacles on flame propagation velocity to properly assess the consequences of Unconfined Vapor Cloud Explosions (UVCE). Within this scope, an UVCE within a congested environment is simulated using RANS modeling of the turbulence. Combustion phenomena are characterized through the progress variable transport equation. The simulation is done with the open source library OpenFoam®. Numerical results are compared with data from the INERIS and GDF-SUEZ experimental campaign EXJET (hydrogen-air and methane-air explosions).

Keywords: *hazards, industrial explosions, CFD, premixed combustion*

1 Introduction

Unconfined Vapor Cloud Explosion (UVCE) is one of the most devastating industrial accidents possible (J. Daubech (2016)). The loss of containment of a flammable product (e.g. methane or hydrogen) can lead to the formation of a flammable cloud all across the plant. The resulting mixture can be lit by any energy source within the cloud (e.g. sparkles, hot surfaces). The propagation of the flame front within the cloud can cause damaging pressure effects in close and long range. In order to assess these damages, CFD can be used, in parallel with widely used phenomenological tools. The open source code OpenFoam® has already been used for such purpose (Bauwens et al. (2011), Ghasemi et al. (2014), Rao et al. (2018)). The global aim of this study is to improve numerical methods for CFD simulation of industrial UVCE.

Hazardous consequences of UVCE are mainly caused by the over-pressure generated by the propagation of the flame front. In deflagration cases, this over-pressure is directly linked to the flame front propagation speed (J. Daubech (2016)). In an industrial configuration, the flame front is impacted by the various obstacles in its way (e.g. pipes, walls). One of the consequences of the presence of obstacles is an acceleration of the flame front (Moen et al. (1980), Moen et al. (1982)) and, consequently, many experiments has been conducted to evaluate this effect. The EXJET campaign (INERIS, GDF-SUEZ) has been set to study experimentally the effect of an obstacle module on the propagation of a flame front in many configurations (steady flammable mix, methane-air jet, hydrogen-air jet).

2 Description of the experimental work

The experimental work considered here has been carried out by INERIS and GDF-SUEZ (Sail et al. (2014)). The aim of the experiment was to study methane jet explosion in a congested environment. The congestion module was a medium size (3m×1m×0.45m) obstacle module, consisting of 296 steel tubes of 2cm diameter. In the framework of the EXJET experimental setup, several experiments have been carried out : methane jet dispersion within the module (without ignition), methane jet ignition within the module, and ignition of a steady methane-air mix. The steady methane-air mix

ignition configuration has been simulated with OpenFoam® in this study.

To assess the pressure variations, several pressure probes are positioned in and around the obstacle module as in Fig. 1. The pressure signals from those probes will be compared to the pressures signals from virtual probes of the numerical simulation. Moreover, pictures of the experiment will be post-process to obtained experimental flame position data.

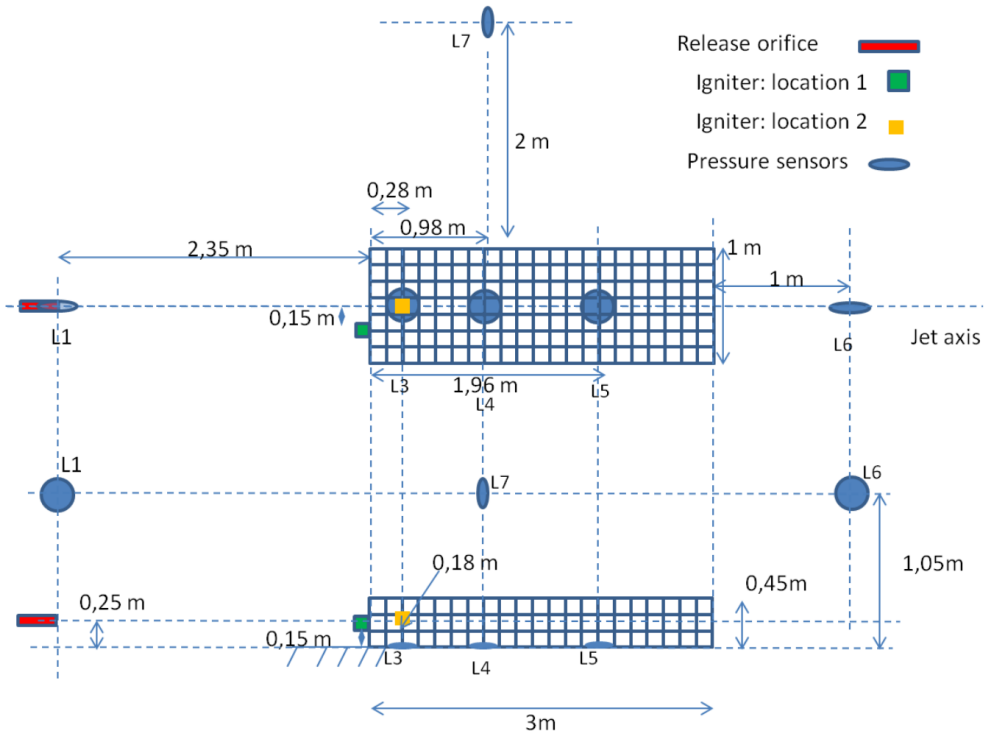

Fig. 1*: Locations of the release orifice, pipes, igniter and pressure sensors used by INERIS and GDF SUEZ for methane jets within a 3D array of 20 mm diameter tubes (Sail et al. (2014)). Up : top view of the obstacle module ; Bottom : side view of the obstacle module.*

In the configuration that interests us, a homogeneous stoichiometric methane-air mixture is spread within the obstacle module. The mixture is kept in the obstacle area by a plastic sheet supported by steel frames. Those plastic sheets will come off with the explosion. The flammable mix is ignited by an electrical ignition device (location 1 on Fig. 1) located inside an aluminium box (19cm×15cm×13cm) with an opening toward the congestion module.

3 Numerical study

3.1 Equations solved

With the solver XiFoam of OpenFoam® v7.0, the Weller b-Xi model (Weller et al. (1998)) is used to model partially premixed combustion. Navier-Stokes equations (eqs. 1, 2) are solved as well as the energy equation (eq. 3).

$$\frac{\partial \overline{\rho}}{\partial t} + \nabla.(\overline{\rho}\widetilde{U}) = 0 \tag{1}$$

$$\frac{\partial \overline{\rho}\widetilde{U}}{\partial t} + \nabla.(\overline{\rho}\widetilde{U}\widetilde{U}) = -\nabla.(\overline{\rho}\widetilde{U''U''}) - \nabla\overline{p} + \nabla.(\overline{\tau}) \tag{2}$$

$$\frac{\partial \overline{\rho}\widetilde{h_t}}{\partial t} + \nabla.(\overline{\rho}\widetilde{U}\widetilde{h_t}) + \frac{\partial \overline{\rho}K}{\partial t} + \nabla.(\overline{\rho}\widetilde{U}K) + \frac{\partial p}{\partial t} + \nabla.(\alpha\nabla\widetilde{h_t}) = \dot{Q} \tag{3}$$

With K being the kinetic energy, α the thermal diffusivity, τ the viscous stress tensor and $\dot{Q}$ an external energy source term (in our case, $\dot{Q} = 0$).

In order to model the combustion, a combustion regress variable "b" is defined (4).

$$b = \frac{T_b - T}{T_b - T_u} \tag{4}$$

With T_b the burnt gases temperature, and T_u the unburnt temperature. A transport equation is solved for this regress variable (5) in order to model the propagation of the flame front.

$$\frac{\partial \overline{\rho} b}{\partial t} + \nabla.(\overline{\rho}\widetilde{U}b) - \nabla.(\alpha \nabla b) = -\rho_u S_u \Xi \mid \nabla b \mid \tag{5}$$

With Su the laminar flame speed, ρ_u the unburnt gases density, and Ξ the flame wrinkling factor (turbulent and laminar flame speed ratio). This ratio is obtained algebraically (6).

$$\Xi = 1 + 2(1-b)\Xi_{coeff}\sqrt{\frac{u'}{Su}R_\eta} \tag{6}$$

With R_η the Kolmogorov Reynolds number, u' the sub-grid turbulence intensity and Ξ_{coeff} a model constant equal, in our case, to 0.62. And finally, to take into account the inhomogeneity of the mix, an equation for a mix variable f_t is solved (7).

$$\frac{\partial \overline{\rho} f_t}{\partial t} + \nabla.(\overline{\rho}\widetilde{U}f_t) = \nabla.(\mu \nabla f_t) \tag{7}$$

With μ the dynamic viscosity. The effects of equivalence ratio inhomogeneity on the flame front propagation speed is taken into account by the S_u term in the b equation with the Gulder flame speed correlation (8) (Gulder (1984)).

$$Su(T, p, \phi) = W\phi^\eta e^{-\xi(\phi-\sigma)}(\frac{T}{T_0})^\alpha(\frac{p}{p_0})^\beta \tag{8}$$

With W, η, σ, α, β Weller model constant and ϕ, the equivalence ratio, being recovered from f_t and $(\frac{Y_{air}}{Y_{fuel}})_{sto}$, the stoichiometric air-fuel ratio .

$$\phi = (\frac{Y_{air}}{Y_{fuel}})_{sto}\frac{f_t}{1-f_t} \tag{9}$$

The ignition is managed via an OpenFoam® integrated module which generate, in a given duration, a spherical volume of burnt gases of a given radius, at a given location. The duration and radius of this ignition kernel has been tuned to the laminar flame speed of the mix.

The PIMPLE algorithm is used to solve the pressure-velocity coupling in XiFoam (Holzmann (2019)). The equations modeling the effect of the combustion are included in the PIMLE loop.

3.1.1 Mesh, boundary condition and numerical schemes

The meshing process has been conducted with both SALOME and the OpenFoam® utilities blockMesh and snappyHexMesh. The domain consists of 836 296 cells and the minimum dx of a cell is 6.25 mm.

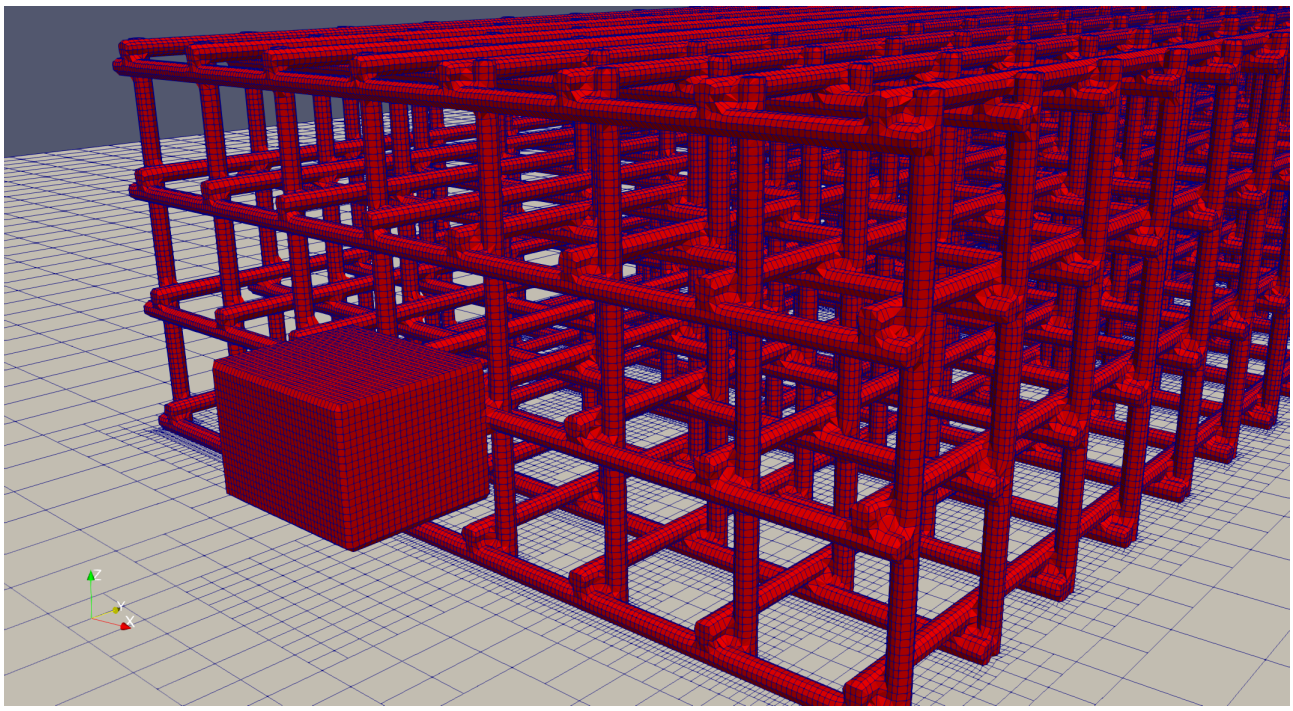

***Fig. 2**: View of the calculation mesh (ParaView)*

The boundary of the numerical domain surrounding the obstacle module is at 2.5m distance of the module in the x and y direction and at 1.5m distance of the module in the z direction.

The boundary conditions to take into account for this simulation are :

- the obstacle module
- the ground
- the ambiant air

The obstacle module and ground will be considered "wall" boundary condition whereas ambient air will be considered free outlet boundary condition. The boundary conditions used are given in Table 1.

***Table 1**: Numerical simulation boundary conditions*

Variable	**WallBC**	**AirBC**
U	fixedValue (0 0 0)	fluxCorrectedVelocity
p	zeroGradient	totalPressure
*	zeroGradient	zeroGradient

The different numerical schemes available in OpenFoam® are detailed in (Moukalled et al. (2015)). The schemes used in this simulation are given in Table 2.

***Table 2**: Simulation numerical schemes*

Variable	**ddt**	**div**	**laplacian**
U/p/k	Euler backward	Upwind	Gauss linear corrected
b/ft	Euler backward	Gauss linearlimited01	Gauss linear corrected
*	Euler backward	Gauss linearlimited	Gauss linear corrected

4 Results and discussion

As we are willing to assess for the over-pressure effects of the UVCE, we will look at two aspects of it : the propagation speed of the flame front and the resulting over-pressure.

4.1 Flame speed

A first simulation has been done to check that the solver take into account the accelerating effect of the obstacles on the flame front. A flame front has been propagated in two cases, with and without an obstacle module. The same mesh and numerical schemes has been used for the two simulation.

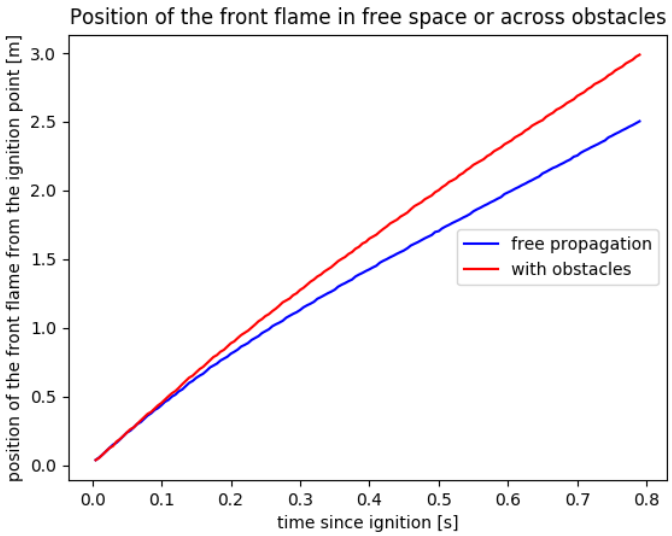

***Fig. 3**: Flame front position in time with and without obstacles*

Here we can see that the flame front positions diverged. An accelerating effect of the obstacle can be observed with XiFoam. We can explain that effect by the turbulent kinetic energy generated by the obstacles. In fact, the flame front propagation, by pushing the fresh gases in front of it, generate a velocity flow normal to the flame surface. This flow, in presence of obstacles, will increase turbulent kinetic energy around those obstacles. This turbulent kinetic energy will, as we can see in (eq .6), increase the wrinkling factor and hence the flame propagation speed, as we can see in (eq. 5). The turbulent kinetic energy generation by the obstacles is illustrated in Fig. 4. There we can see that turbulent kinetic energy is generated around the obstacles crossed by the flame front.

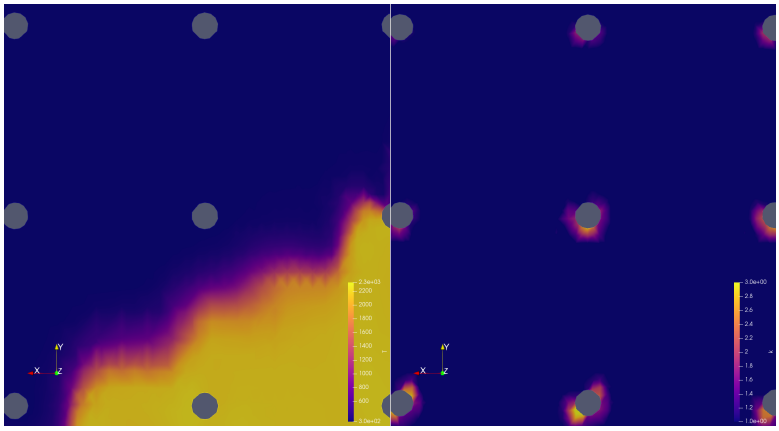

***Fig. 4**: Sectional view (z axis) of the flame front propagation (Paraview). Left : temperature (K), right : turbulent kinetic energy ($m^2.s^{-2}$)*

Finally, we can compare the experimental and numerical flame speed. We observe an acceleration of the experimental flame front during the whole experiment, starting propagating at 9 m/s until it attained a speed of roughly 25 m/s. In the numerical case however, we observe a constant flame speed of approximately 12 m/s. As we are in the same magnitude in term of flame propagation speed, we fail to reconstruct the accelerating behavior of the flame front within the obstacle module. The usage of a transport equation for Ξ in further work can be a lead toward reproducing this accelerating behavior.

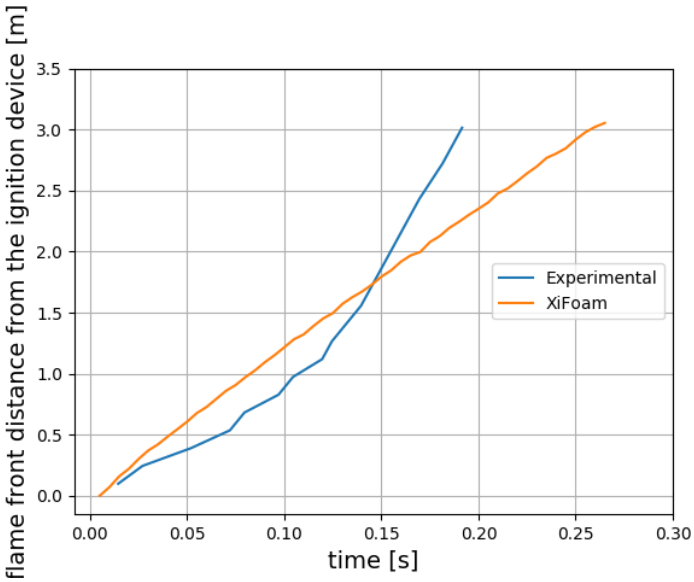

***Fig. 5**: Experimental and numerical flame front position from the ignition point in time*

4.2 Pressure signal

For the pressure signals, the numerical simulation result in an over-pressure "wave" being pushed by the flame front, as shown on the Fig. 6. There we can observe an over-pressure "wave" just in front of the flame front. This over-pressure is the result of the unburnt gases being pushed by the flame front propagation.

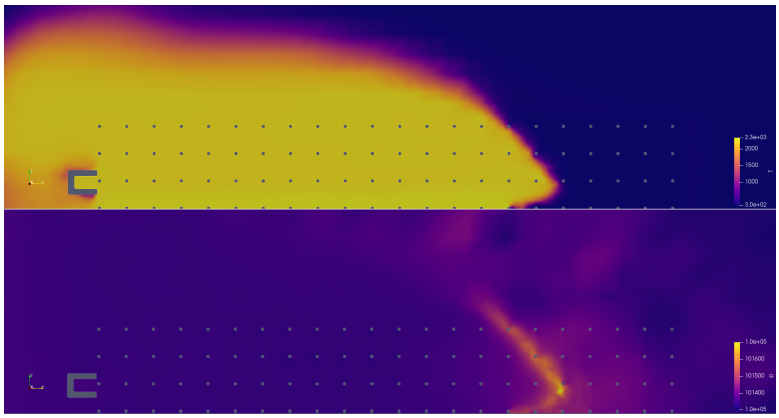

***Fig. 6**: Sectional view (x axis) of the flame front propagation at t = 0.2 sec (Paraview). Up : temperature (K), down : pressure (Pa)*

But when comparing the signals from two pressure probes (positioned along the y axis from the ignition point) Fig. 7, both experimental and numerical, we couldn't reproduce with precision the over-pressure wave. There we can see that at 0.28 cm from the ignition point, a 4.5 mmBar over-pressure is obtained but the peak is obtained numerically at approximately 0.03sec in the numerical

case, versus 0.1sec for the experimental case. However, with the over-pressure being "pushed" by the flame front, the phase between the two signal is likely to be induced by the different position of the experimental and numerical flame front.

Now at 1.96m from the ignition point, the two over-pressure peaks are occurring approximately at the same time (0.16 sec), but the magnitude is not accurately reproduced. The numerical over-pressure peak value is 1.75 mmBar and the experimental one being 6 mmBar. This difference may be explained by the flame speed difference when crossing the probe. In fact, at the moment where the flame crosses the probe at 1.96m from the ignition point, the experimental has already attained its max velocity of 25 m/s whereas the numerical one is still at the same speed of 12 m/s Fig. 5.

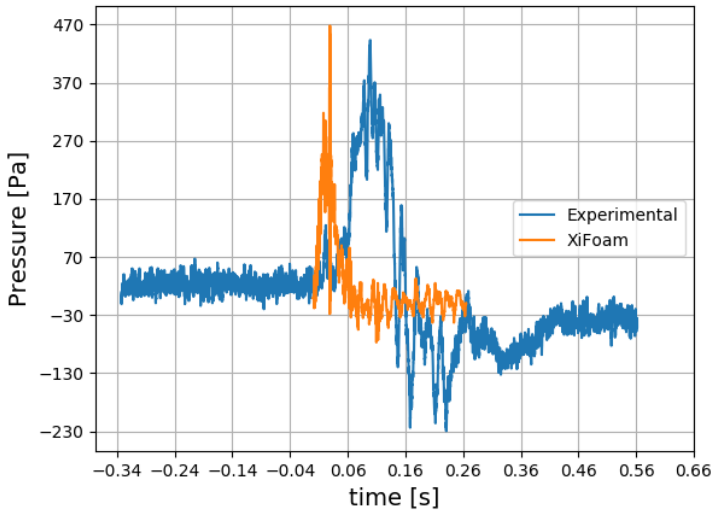

(a) Relative pressure at 0.28m from the ignition point

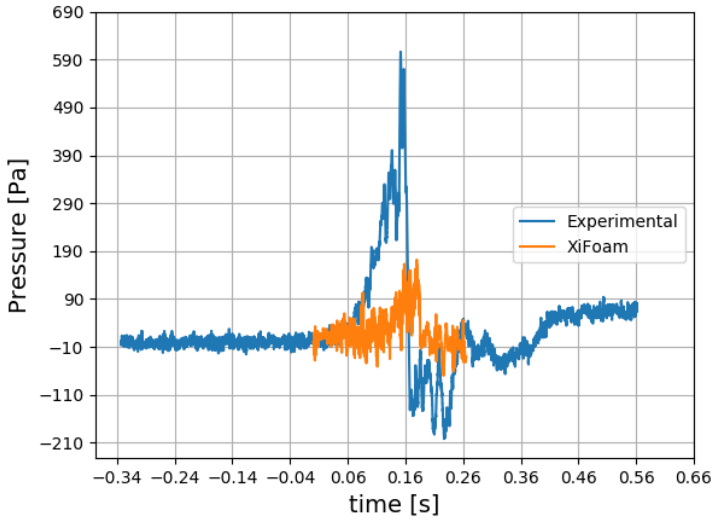

(b) Relative pressure at 1.96m from the ignition point

***Fig. 7**: Relative pressure signal in time at 2 point on the y axis*

The magnitude of the peak over-pressure is roughly the same (severals mBar), although the over-pressure is attenuated between the two probes for the numerical simulation(from 4.7 mBar to 1.8 mBar), and is enhanced in the experiment(from 4.5mBar to 6.0 mBar). This is probably explained by the acceleration of the experimental flame front Fig. 5 between the two probes, effectively generating more over-pressure in front of it.

5 Conclusions

In this study, a methane-air explosion in a confined environment has been simulated. The explosion "at rest" case of the EXJET (INERIS GDF-SUEZ) as been taken to assess for the fidelity of the simulation with OpenFoam®. So far, several aspects of the simulation have shown good agreement with the experiment : The accelerating effect of the obstacles can be reproduced, and magnitude of both flame speed and over-pressure peaks are conserved. But the study fails to reproduce the accelerating behavior of the flame front and hence the over-pressure signals obtained numerically are not accurately reproducing the experimental ones.

The key to reproduce with fidelity the over-pressure signals (and more specifically, the over pressure peak values) is to capture with fidelity the flame propagation speed. Current works on the transport equation for Ξ are carried out to take care of that aspects. Results will be updated accordingly.

References

Bauwens, C., Chaffee, J., Dorofeev, S. (2011). *Vented explosion overpressures from combustion of hydrogen and hydrocarbon mixtures*. International Journal of Hydrogen Energy, 36(3):2329 – 2336. ISSN 0360-3199. doi:https://doi.org/10.1016/j.ijhydene.2010.04.005. The Third Annual International Conference on Hydrogen Safety.

Ghasemi, E., Soleimani, S., Lin, C. (2014). *Rans simulation of methane-air burner using local extinction approach within eddy dissipation concept by openfoam*. International Communications in Heat and Mass Transfer, 54:96 – 102. ISSN 0735-1933. doi: https://doi.org/10.1016/j.icheatmasstransfer.2014.03.006.

Gulder, O. (1984). *Correlations of laminar combustion data for alternative si engine fuels*.

Holzmann, T. (2019). *Mathematics, Numerics, Derivations and OpenFOAM®*.

J. Daubech, E. Leprette, C. P. (2016). *Formalisation du savoir et des outils dans le domaine des risques majeurs (eat-dra-76) les explosions non confinées de gaz et de vapeurs - ω uvce*. Technical report, Institut National de l'Environnement Industriel et des Risques.

Moen, I., Donato, M., Knystautas, R., Lee, J. (1980). *Flame acceleration due to turbulence produced by obstacles*. Combustion and Flame, 39(1):21 – 32. ISSN 0010-2180. doi: https://doi.org/10.1016/0010-2180(80)90003-6.

Moen, I., Lee, J., Hjertager, B., Fuhre, K., Eckhoff, R. (1982). *Pressure development due to turbulent flame propagation in large-scale methaneair explosions*. Combustion and Flame, 47:31 – 52. ISSN 0010-2180. doi:https://doi.org/10.1016/0010-2180(82)90087-6.

Moukalled, F., Mangani, L., Darwish, M. (2015). *The Finite Volume Method in Computational Fluid Dynamics: An Advanced Introduction with OpenFOAM® and Matlab®*, volume 113. ISBN 978-3-319-16873-9. doi:10.1007/978-3-319-16874-6.

Rao, V. C. M., Sathiah, P., Wen, J. X. (2018). *Effects of congestion and confining walls on turbulent deflagrations in a hydrogen storage facility-part 2: Numerical study*. International Journal of Hydrogen Energy, 43(32):15593 – 15621. ISSN 0360-3199. doi: https://doi.org/10.1016/j.ijhydene.2018.06.100.

Sail, J., Blanchetiere, V., Geniaut, B., Osman, K., Daubech, J., Jamois, D., Hebrard, J. (2014). *Review of knowledge and recent works on the influence of initial turbulence in methane explosion*. In SKJOLD, T., ECKHOFF, R. K., VAN WINGERDEN, K., editors, *10. International symposium on hazards, prevention, and mitigation of industrial explosions (X ISHPMIE)*, pages 401–432. GexCon AS, Bergen, Norway.

Weller, H., Tabor, G., Gosman, A., Fureby, C. (1998). *Application of a flame-wrinkling les combustion model to a turbulent mixing layer*. Symposium (International) on Combustion, 27(1):899 – 907. ISSN 0082-0784. doi:https://doi.org/10.1016/S0082-0784(98)80487-6. Twenty-Seventh Sysposium (International) on Combustion Volume One.